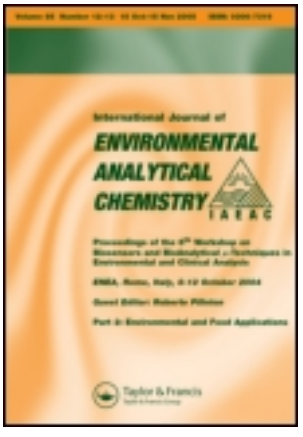

International Journal of Environmental Analytical Chemistry

Publication details, including instructions for authors and subscription information:
http://www.tandfonline.com/loi/geac20

Modelling assessment of carbon supply by different macrophytes for nitrogen removal in pilot vegetated mesocosms

Renato Iannelli [a], Veronica Bianchi [a], Michela Salvato [b] & Maurizio Borin [b]

[a] Department of Civil Engineering, University of Pisa, Via Gabba 22, 56122 Pisa, Italy

[b] Department of Environmental Agronomy and Vegetable Production, University of Padova, Viale dell'Università 16, Legnaro, 35020 Padova, Italy

Available online: 16 May 2011

To cite this article: Renato Iannelli, Veronica Bianchi, Michela Salvato & Maurizio Borin (2011): Modelling assessment of carbon supply by different macrophytes for nitrogen removal in pilot vegetated mesocosms, International Journal of Environmental Analytical Chemistry, 91:7-8, 708-726

To link to this article: http://dx.doi.org/10.1080/03067319.2011.557159

Intern. J. Environ. Anal. Chem.
Vol. 91, Nos. 7–8, 15 June–15 July 2011, 708–726

Taylor & Francis
Taylor & Francis Group

Modelling assessment of carbon supply by different macrophytes for nitrogen removal in pilot vegetated mesocosms

Renato Iannelli[a]*, Veronica Bianchi[a], Michela Salvato[b] and Maurizio Borin[b]

[a]*Department of Civil Engineering, University of Pisa, Via Gabba 22, 56122 Pisa, Italy;*
[b]*Department of Environmental Agronomy and Vegetable Production, University of Padova, Viale dell'Università 16, Legnaro, 35020 Padova, Italy*

(*Received 13 January 2010; final version received 19 January 2011*)

The aim of this study was the evaluation of carbon supply by different macrophytes for nitrogen removal in constructed wetlands, using a dynamic numerical model previously developed by our work group to assess the results of a recently published meso-scale experiment. The experiment consisted of 12 mesocosms (five different macrophytes plus an unvegetated control, two cells each) drained once a week and immediately fed again until complete submersion with a solution of ammonium nitrate. To leave out any external carbon supply, no carbon substrate was added to the feed flux and no organic soil was included in the support media. The numerical simulations were obtained by calibration of the nitrification and denitrification processes driven by the alternate aerobic-anoxic phases generated by the weekly filling–emptying cycles. The carbon supplied by plants was demonstrated to be the main parameter affecting the denitrification rates observed in the experiments. It ranged in summer from 5.76 to 7.02 g/(m^2 d), while the control accounted for 5.11 g/(m^2 d). A winter test showed a 54% reduction of the summer supply of the same plant. The observed evapotranspiration rates were also simulated, and were shown to significantly affect the behaviour of the mesocosms planted with different species. Finally, the different vertical root-density distributions of the plants were found to play a relevant role in the development of nitrogen removal.

Keywords: sub-surface constructed wetlands; nitrification; denitrification; macrophytes; modelling

1. Introduction

Constructed wetlands (CWs) have become an accepted technology in a wide range of situations as a self-sufficient option for treating municipal, industrial, and agricultural wastewater or urban stormwater [1], as well as a polishing or tertiary treatment option for conventional treatment plants [2,3].

Among the several available types of treatment CWs, subsurface-flow (SSF) wetlands rely on a wastewater flux filtering through a sand or gravel medium that acts as a support for the planted macrophytes [4].

The most commonly applied type of SSF CW adopts a horizontal subsurface flux and is widely used as a simple, efficient, reliable, and cost-effective secondary technique for small civil communities, requiring minimal operational attention [5].

*Corresponding author. Email: r.iannelli@ing.unipi.it

ISSN 0306–7319 print/ISSN 1029–0397 online

DOI: 10.1080/03067319.2011.557159
http://www.informaworld.com

The second type of SSF CW is the so-called vertical flow (VF) CW, for which a number of sub-types are available involving intermittent or continuous unsaturated down-flow, saturated up- or down-flow, and fill-and-drain cycles (tidal flow) [6]. All of these types, which often involve a higher level of required technology (namely siphons or pumps to obtain the required feed-drain pulses and/or recirculation fluxes), are mainly aimed at improving the aeration efficiency to obtain more compact installations, or to improve the removal of nitrogen [7].

Unlike in other fields of technology, numerical modelling has rarely been applied to simulate CW behaviour. To design the installations, simplified equations have commonly been used, relying on parameters that are largely specific to different regions and climates. This fact is mainly attributed to the complexity of the involved physical and bio-chemical phenomena, that make the models particularly complex and difficult to calibrate. Furthermore, since CWs are in most cases applied to small and simple installations, the available operational data are generally insufficient for the proper calibration of detailed numerical models.

Nevertheless, the potential use of numerical modelling to gain a better understanding of the processes involved in CWs and for improving their design and operational criteria, has recently been highlighted by several authors [8–11].

Until now, only a few complete numerical models have been developed to simulate CW systems, and most of these are dedicated to horizontal-flow systems [10,11]. Conversely, our group recently presented a numerical model named FITOVERT, expressly developed to simulate the typically unsteady behaviour of VF-CWs.

This model is based on the dynamic multi-component reactive transport numerical simulation of partial saturation with a volume filtration of particulates. A brief presentation of its features is reported in the Section 2.2 of the present paper, while further details can be found in the dedicated paper [9].

Since the enhanced removal of nitrogen is one of the main goals of VF-CWs, an accurate simulation of the N transformation and removal processes is among the most important features of a good VF-CW simulation model. A number of processes are reported to contribute to the transformations of the various forms of N in CWs [6]. Specifically, the following processes have been recognised:

- physical processes: adsorption-desorption, volatilisation, sedimentation, atmospheric deposition;
- biochemical processes: ammonification, nitritation, nitrification, denitrification, dissimilatory reduction, anaerobic ammonia oxidation, fixation;
- vegetation driven processes: plant uptake, accretion.

Depending on the circumstances, only few of the processes listed above are recognised as playing a significant role. While the effect of plant uptake can be significant during the early stages of newly built CWs [6], in well-established beds the seasonal effect of plant uptake is considered negligible in most cases [12] as are the other physical and vegetation driven processes. Hence, the most active processes in N removal are those involved in the microbial-driven chain of ammonification, nitritation, nitrification, and denitrification [13].

Since nitritation and nitrification are strictly aerobic, whereas denitrification is strictly anoxic and requires a source of readily available organic carbon, these processes are recognised as being mainly governed by the presence of oxygen and carbon.

Regarding oxygen, some VF wetlands (namely the intermittent or continuous unsaturated down-flow CWs) are engineered in such a way that largely aerobic conditions are provided, thus specialising them in nitrification processes, whereas others (mainly tidal flow CWs) are aimed at allowing aerobic-anoxic cycles so as to promote both nitrification and denitrification.

As for the carbon source, a number of treatment wetland studies have demonstrated the effectiveness of plant biomass addition [14], methanol [15], acetic acid [16], potato processing water [17], and other carbon sources. However, external carbon supplements are not commonly provided in CWs, and the most important sources of organic carbon for denitrification are the influent RBCOD (readily biodegradable chemical oxygen demand), when available in sufficient amounts, the decomposition of tissues, and the exudates by living roots [18]. The ability to provide significant amounts of C by living root exudates is a desirable feature that makes some plants particularly feasible for CWs aimed at maximising the removal of nitrogen [12]. This feature is worth considering in the debated role of plants in CW performances [19,20].

2. Experimental

An experimental mesocosm-scale study was conducted by our work group with the aim of assessing the ability of four different macrophyte species to remove N in the complete absence of any external C source. The main data obtained from the experiments and statistical analysis of the results have been published recently [21].

Since the mass balance of N, including the evaluation of its storage in vegetal tissues, showed a secondary role of plant uptake in the observed overall removal, a deeper analysis of N removal by nitrification–denitrification was required. This was conducted using FITOVERT simulations, and is presented in this paper. This analysis allowed us to focus on the role of different macrophytes in the processes involved in nitrogen removal.

2.1 *Meso-scale experiment*

The reference data were collected from an experimental installation built in Padova (northern Italy: 45°42′N, 11°88′E; mean daily temperature ranging from −5° to 6°C in the winter and from 18° to 28°C in the summer) comprising 12 tanks of 50 L and 0.2 m^2 each. Each tank was equipped with a bottom drainage tap, was filled with gravel ($d_{10\%} = 4$ mm; $d_{95\%} = 7$ mm), and was kept in a cold glasshouse from October 2006 to March 2008. Ten tanks were planted in October 2006 (two tanks per species, six plants per tank) with *Carex elata All.*, *Juncus effusus* L., *Phragmites australis* (*Cav.*) *Trin.*, *Phalaris arundinacea* L. var. *picta*, and *Typha latifolia* L. The last two tanks were left unplanted as the controls.

From January to July 2007, each tank was filled every 4 weeks with 12 L of ammonium nitrate solution ($NO_3^- = 52$ mg/L N; $NH_4^+ = 56$ mg/L N) so as to saturate the whole gravel bed. From August 2007 to February 2008 the concentration was doubled. These concentrations were chosen after an approximate estimation of the highest values that did not cause any possible adverse effect to any of the plant species.

At the end of each week, each tank was drained by opening the bottom tap. The drained solution was collected, analysed for NO_3^- and NH_4^+ concentrations, and used to refill the same tank after measuring its volume and compensating for the evapotranspiration loss with an equivalent amount of freshwater. Air and water temperatures, plant

heights, and shoot densities were also measured during the experiments. The analyses were performed using a portable spectrophotometer (DR2800, Hach Lange, Germany) immediately after collecting the water samples. The concentration of NH_4^+ was detected using Laton cuvette tests LCK 302 and 303 based on indophenol blue colorimetry according to standard method 4500-NH3 [22] and the concentration of NO_3^- using Laton cuvette tests LCK 339 and 340 based on 2,6-dimethylphenol colorimetry according to standard method 4500-NO3 [22].

At the end of the experiments the 12 mesocosms were destroyed in order to observe the final root density for each plant species.

Further details on the materials and methods used for this experimentation are reported in [21], as well as the complete obtained dataset and its statistical analysis.

2.2 *The mathematical model used*

The mathematical model used to simulate the CW installation was a dynamic multi-component reactive transport model for partial saturation that was recently presented by our research group [9]. It simulates a SSF-CW as a series of vertically stacked layers (vertical 1D topology) by solving an extended set of linked partial-derivatives differential equations grouped in the following modules:

(i) hydraulic module: this simulates the vertical water flow through a porous medium in unsaturated conditions using the Richards equation with van Genuchten-Mualem constitutive functions and parameters [9];
(ii) biochemical module: this describes the fate of 13 components representing the various dissolved and particulate forms of organic carbon and nitrogen by eight interconnected bio-kinetic processes. It is based on the ASM1 modelling structure [23,24] originally developed to simulate the activated sludge process;
(iii) transport of dissolved components: this simulates the advective-dispersive transport of soluble components in the liquid phase according to Bresler's equation [9];
(iv) transport of particulate components: this uses an original filtration model based on the Iwasaki-Ives scheme [9] and is able to account for changes of porosity and hydraulic conductivity due to solids and biofilm accumulation;
(v) oxygen transfer: this separately simulates the advective and diffusive transport of oxygen in the gaseous phase and its transfer to the liquid phase of the soil by Fick's law with the diffusion coefficient corrected by way of a tortuosity factor accounting for the properties of the soil and the contribution of the macrophytes;
(vi) evapotranspiration: this accounts for surface water losses owing to evaporation, and deep water losses due to transpiration, which, in turn, is related to root density and the leaf area index.

It should be noted that the processes of nitritation and nitrification are merged within a single process in the ASM1 biochemical simulation structure. Hence, the presence of nitrites is neglected.

The endogenous supply of a readily available C source was assumed to be transferred to the system by the roots of the plants. It was simulated as a continuous provision of readily biodegradable chemical oxygen demand (RBCOD) uniformly fed along the whole

depth of the bed, proportionally to the vertical distribution of plant-root density. The rate of provision was attributed to diffusion from the roots to the soil. Therefore, it was simulated as an increment of concentration by the following equation:

$$r_{EC}(z) = r_{ECtot} \cdot RD_Z(z)$$

where:

z = the vertical coordinate of the bed (cm);
$r_{EC}(z)$ = the increment of C concentration provided by the roots (mg RBCOD $L^{-1} s^{-1}$), variable along the vertical coordinate;
r_{ECtot} = the overall increment of C concentration provided by the roots (mg RBCOD $L^{-1} s^{-1}$);
$RD_Z(z)$ = the dimensionless vertical distribution of the root density, calculated in such a way that $\int_0^{Hbed} RD_z(z)dz = 1$, with H_{bed} = total height of the bed.

Since the vertical distribution of root density RD_Z was assumed to be trapezoidal, the implemented calibration parameters were the maximum depth reached by the roots (Z_{max}), the minimum and maximum depths of the central part or the root system with constant density (Zs_{max1} and Zs_{max2}, respectively) and the overall RBCOD provision (r_{ECtot}). The three parameters describing the vertical distribution of the roots were estimated for each plant species based on the actual root density distribution observed at the end of the experiment. The overall RBCOD provision was calibrated by a "trial and error" method, as described in Section 2.5.

The same vertical distribution of root density was also used to calculate the transpiration loss, which was assumed to be extracted along the vertical direction, in proportion to the vertical distribution of the root density.

2.3 *Boundary conditions and initial conditions*

Even though the model was conceived to simulate VF-CWs, its application in this experiment was possible despite the significant differences between the experimental mesocosms and typical full-scale VF-CWs. In fact, the experimental mesocosms were intermittently fed from the top and drained from the bottom, similar to VF-CWs.

Tank filling, performed by manually pouring water onto the surface of each mesocosm at the beginning of each week, was simulated as a constant flux entering the bed from the top for a duration of 30 min. The length of this duration was longer than the duration used in the simulated experiment to manually pour the water into the mesocosms, but it was shorter, by an order of magnitude, than the subsequent duration of one week of no feeding. Using this length of duration avoided the generation of a "stiff" numerical problem (which would have added convergence problems and significantly increased the simulation time), while maintaining an acceptable correspondence with the filling procedure used in reality.

Tank drainage, performed at the end of each week by opening the bottom tap for a few minutes until complete drainage, was simulated by applying the boundary condition of atmospheric pressure for 30 min at the bottom of the computational field. The rest of the week was simulated via boundary conditions of null flux at the top and at the bottom of the computational field, resulting in the retention of water with the only exception of being loss owing to evapotranspiration.

The composition of the feed water was input as a set of boundary conditions. The concentrations of dissolved oxygen, ammonium, and nitrate measured in the feed water were input in the model, keeping all of the other nine components of the ASM1 scheme null, since they were actually in the water used to feed the cells.

The carbon required for denitrification was assumed to be provided by the plant. For its estimation, the parameters describing the vertical distribution of the root density were deducted from the actual root densities observed for the different plants at the end of the experiment. The rate of C provision r_{ECtot} was used to calibrate the effect of denitrification by the "trial and error" approach described in Section 2.5.

The average temperature and relative humidity measured during the experiment were used as boundary condition for evapotranspiration modelling.

The initial conditions of the calibration runs were prepared by running a preliminary simulation of one month, starting from a clean bed, and using the final state of the bed as the initial condition for the proper simulation. This duration was sufficient for the formation of an amount of biota able to provide a N removal rate comparable to that observed during the mesocosm experiments.

2.4 *Data from the meso-scale experiment used for the calibration*

Most of the calibration runs were conducted so as to simulate the first week of July 2007, and the simulation was repeated and calibrated for four of the five plant species used, and for the unplanted control (the simulation of *Phalaris arundinacea* was omitted because the two mesocosms planted with this species showed excessively inconsistent behaviours). For each test, an average of the data detected in the two available mesocosms during the experiment was used. The selected week was chosen because it presented the most complete set of experimental data for the whole pilot experiment, and it was unaffected by errors or data loss. The subsequent week (the second week of July 2007) was used to validate the calibration.

To test the seasonal effect of temperature and vegetation, a winter experiment was simulated as well. Specifically, we simulated the experiment conducted for *Carex elata* in December 2007 with doubled N concentration. Since, in this experiment, the analyses were performed only at the end of the first and fourth week, we used the first week for calibration and the subsequent three weeks for validation.

The outlet concentrations of ammonia and nitrate observed at the end of each week of July 2007 (December 2007 for the winter tests) are reported in Table 1.

Regarding evapotranspiration, the rates of water loss measured in July 2007 are reported in Figure 1. *Typha l.* was the most active plant in terms of evapotranspiration. As expected, the winter loss of *Carex e.* was substantially lower than in summer, and the only summer loss of the control cells was due to evaporation, causing a total water reduction much lower than in the vegetated cells.

2.5 *Calibration and validation of the model*

The model dynamically simulated the time variations of the concentrations of each of the biochemical and physical parameters in each computational element of the bed throughout the entire duration of the simulated experiments. Conversely, the only data available from

Table 1. Nitrate and ammonium concentrations observed in each cell.

	NO_3^- (mg/L N)					NH_4^+ (mg/L N)				
July 2007:	Inlet	Week 1		Week 2		Inlet	Week 1		Week 2	
Carex e.	52.0	52.0	70.0	47.0	69.0	56.0	11.0	14.0	0.00	0.00
Juncus e.	52.0	80.0	95.0	78.0	96.0	56.0	12.0	14.0	0.00	0.00
Phragmites a.	52.0	75.0	73.0	72.0	76.0	56.0	29.0	15.0	0.00	0.00
Typha l.	52.0	122.0	88.0	68.0	78.0	56.0	6.2	6.2	1.00	0.00
Control	52.0	85.0	75.0	100.0	89.0	56.0	15.0	15.0	0.00	0.00
Dec. 2007:	Inlet	Week 1		Week 4		Inlet	Week 1		Week 4	
Carex e.	114.4	159.2	175.6	224.0	232.0	113.0	2.85	2.78	0.00	0.00

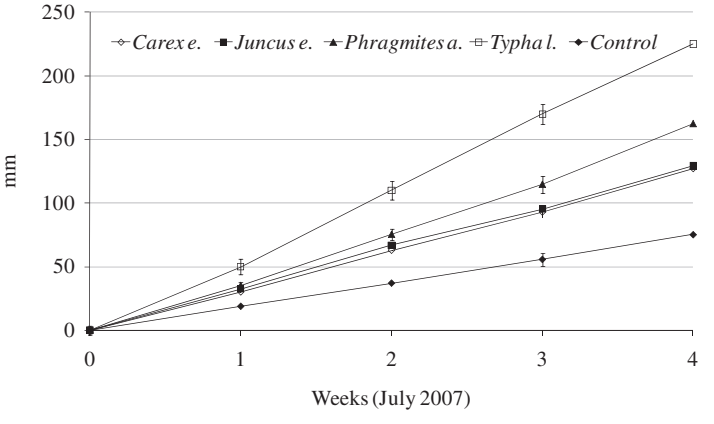

Figure 1. Evapotranspiration losses in July 2007. The values are means of the two data represented by the endpoints of the bars.

the reference experiment were the water volumes and the ammonium and nitrate concentrations measured at the beginning and at the end of the examined weeks.

In order to compare these different sets of values, at the end of each week, immediately before the beginning of the draining procedure, the concentrations of ammonium and nitrate nitrogen calculated for each computational element were averaged, weighting each value to the water volume of the corresponding computational element. These values were compared to the goal values, represented by the concentrations measured in the water drained at the end of each week during the reference experiments.

The calibration was then performed according to a "trial and error" approach. This consisted of repeating the simulations, after correcting a selected subset of calibration parameters, until good simulations of the goals were obtained at the end of the simulated weeks for each plant.

Most of the calibration parameters required by the FITOVERT model were left untouched at their default values (original ASM1 values as suggested by [23] for the

biochemical parameters, and typical gravel soil literature values for the ground parameters). Only a few parameters were adapted with the goal of obtaining, at the end of the simulated weeks, values of water volume, ammonia nitrogen and nitrate nitrogen as close as possible to those detected during the reference experiments.

The calibration parameters used for all the simulations are presented in Table 2. The selected parameters that were adapted to specific values for each cell during the calibration process are presented in Table 3.

The modelling of water loss was calibrated by adjusting the value of the maximum evapotranspiration rate ET_p until a good simulation of the residual water volume detected at the end of the simulated week was reached. Based on the observations conducted at the end of the experiment, the root density distributions of the simulated species (Figure 2) were associated with a rectangular shape for *Phragmites australis* and *Typha latifolia*, and with a trapezoidal shape for *Carex elata* and *Juncus effusus*. For the unplanted control, a triangular distribution was adopted, to account for the observed vegetal biofilm attached to the upper layer of the gravel bed.

After calibration, the model was validated by simulating the subsequent week (three weeks for the winter test). For these simulations, the calibration parameters were left untouched; the final conditions of the calibration tests were used as initial conditions, and the data measured in the validation weeks (input fluxes and concentrations, average air temperature and humidity) were used as boundary conditions.

The removal efficiencies of ammonium and nitrate obtained at the end of the validation runs were compared to the corresponding values measured during the experiments.

To evaluate the "goodness-of-fit" of the removal efficiencies obtained in the validation, five methods were used: the coefficient of determination, the Nash–Sutcliffe coefficient of efficiency, the normalised mean bias error, the normalised root mean square error, and scatter plots of estimated-versus-observed data.

The coefficient of determination R^2 [25] is the square of the Pearson's product-moment correlation coefficient, and describes the proportion of the total variance in the observed data that can be explained by the model. It ranges from 0 to 1, with higher values indicating better agreement, and is given by:

$$R^2 \left\{ \frac{\sum_{i=1}^{N} (O_i - \bar{O})(P_i - \bar{P})}{\left[\sum_{i=1}^{N} (O_i - \bar{O})^2\right]^{0.5} \left[\sum_{i-1}^{N} (P_i - P)^2\right]^{0.5}} \right\}^2$$

where N is the number of simulated data O_i are the observed data, P_i are the simulated data, and the overbars denote the averages of the corresponding data-sets. Specifically, the final predicted removal efficiencies for each plant and for the control were used as simulated data, and the averages of the removal efficiencies measured for the two cells of each plant and of the control were used as observed data.

The Nash–Sutcliffe coefficient of efficiency E [25,26], ranging from minus infinity to 1 with higher values indicating better agreement, is defined as:

$$E = 1 - \frac{\sum_{i=1}^{N} (O_i - P_i)^2}{\sum_{i=1}^{N} (O_i - \bar{O})^2}$$

with the same notations of the previous equation.

Table 2. Default calibration parameters used for all of the cells.

Dispersion coefficient: λ_d (−)	Global coefficient of oxygen exchange: K_{LA} (s^{-1})	Van Genuchten parameters: Pore size distrib. n (−)	Air suction coeff. α (cm^{-1})	Saturation conductivity K_s (cm/s)	Residual water content θ_r (−)	Saturated water content θ_s (−)
10	0.0006	4.02	0.435	0.0495	0.045	0.35

Biochemical parameters:	Symbol	Original ASM1 values [23,24] 20°C	10°C	Range	Adopted values
Stoichiometric parameters:					
Heterotrophic yield (g cell COD formed/g COD oxidised)	Y_H	0.67	0.67	0.38–0.75	0.67
Autotrophic yield (g cell COD formed/g N oxidised)	Y_A	0.24	0.24	0.07–0.28	0.24
Fraction of biomass yielding particulate products (dimentionless)	f_P	0.08	0.08	–	0.08
Mass N/mass COD in biomass (dimentionless)	i_{XB}	0.086	0.086	–	0.086
Mass N/mass COD in products from biomass (dimentionless)	i_{XP}	0.06	0.06	–	0.06
Kinetic parameters:					
Heterotrophic max. specific growth rate (day^{-1})	μ_H	6.0	3.0	0.6–13.2	6
Heterotrophic decay rate (day^{-1})	b_H	0.62	0.20	0.05–1.6	0.62
Half-saturation coefficient (hsc) for heterotrophs ($g\,COD\,m^{-3}$)	K_S	20	20	5–225	20
Oxygen hsc for heterotrophs ($gO_2\,m^{-3}$)	$K_{O,H}$	0.20	0.20	0.01–0.20	0.20
Nitrate hsc for denitrifying heterotrophs ($g\,N\,m^{-3}$)	K_{NO}	0.50	0.50	0.1–0.5	0.50
Autotrophic max. specific growth rate (day^{-1})	μ_A	0.80	0.30	0.2–1.0	0.26÷0.94
Autotrophic decay rate (day^{-1})	b_A	0.20	0.10	0.05–0.2	0.12
Oxygen hsc for autotrophs ($g\,O_2\,m^{-3}$)	$K_{O,A}$	0.4	0.4	0.4–2.0	0.4
Ammonia hsc for autotrophs ($gN\,m^{-3}$)	K_{NH}	1.0	1.0	–	1.0
Correction factor for anoxic growth of heterotrophs (dimentionless)	η_g	0.8	0.8	0.6–1.0	0.8
Ammonification rate ($m^3\,g$ cell $COD^{-1}\,day^{-1}$)	k_a	0.08	0.04	–	0.08
Max. specific hydrolysis rate (g s.b.COD g cell $BOD^{-1}\,day^{-1}$)	k_h	3.0	1.0	–	3.0
Hsc for hydrolysis of slowly biodegr. substrate (g s.b.COD g cell BOD^{-1})	K_X	0.03	0.01	–	0.03
Correction factor for anoxic hydrolysis (dimentionless)	η_h	0.4	0.4	–	0.4

Table 3. Plant specific parameters after calibration of the model.

Plant	Endogenous carbon provision		Vertical distribution of root density (cm)			Autotrophic maximum specific growth rate μ_A (d^{-1})	Potential evapotraspiration rate ET_p (mm/d)
	Supply rate r_{ECtot} ($mg\,L^{-1}\,s^{-1}$)	Calculated average ($g\,m^{-2}\,d^{-1}$)	Z_{max}	Zs_{max1}	Zs_{max2}		
July 2007:							
Carex e.	0.032	6.73	24	0	12	0.80	5.5
Juncus e.	0.028	5.89	24	0	12	0.90	5.5
Phragmites a.	0.031	7.02	24	0	24	0.70	6.3
Typha l.	0.027	5.76	24	0	24	0.94	8.0
Control	0.023	5.11	24	0	0	0.80	3.0
December 2007:							
Carex e.	0.009	3.08	24	0	12	0.26	0.54

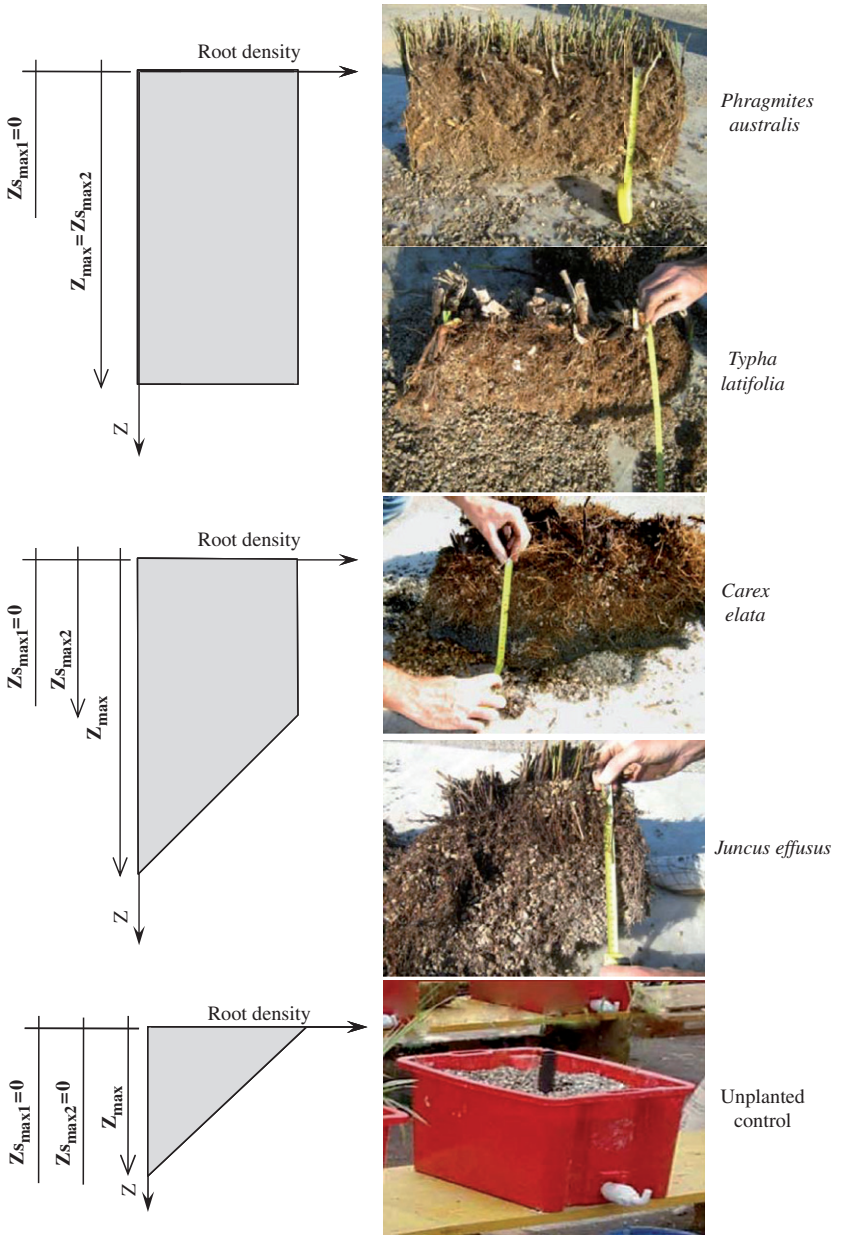

Figure 2. Assumptions for the vertical distribution of the root density of the plants.

The normalised mean bias error (NMBE) and normalised root mean square error (NRMSE) tests are defined as below [27]:

$$NMBE = \sum_{i=1}^{N} (P_i - O_i)/N; \quad NRMSE = \sqrt{\sum_{i=1}^{N} (P_i - O_i)^2/N}$$

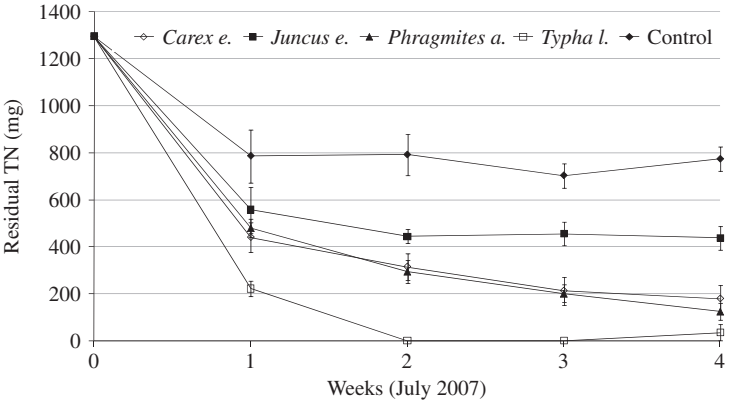

Figure 3. Total N residues detected in July 2007. The values are means of the two data represented by the endpoints of the bars.

with the same notations of the previous equations. NMBE belongs to real numbers, with negative values close to zero indicating better agreement, and a positive value giving the mean amount of overestimation of an individual observation cancelling an underestimation in a separate observation. NRMSE belongs to positive real numbers, with lower values indicating better agreement.

The scatterplots of estimated-versus-observed data allow a visual estimation of the goodness of fit, with the aid of the line of perfect agreement (corresponding to the bisector of the first and third quadrant of the scattergram) and couples of lines representing prefixed ranges of deviation from the perfect agreement.

3. Results and discussion

3.1 *Nitrogen mass balance of the experimental data*

During the whole experiment, high removal efficiencies of ammonium (83–100%, depending on the cells) were constantly observed within one month of application for all the cells, including in the unplanted control. The removal of ammonium was maximum (99–100%) in July 2007, the warmest month of the observation period. As explained later, the rapid ammonium removal also observed in winter was due to adsorption by the gravel medium.

Conversely, wide ranges of variability were observed for the removal of nitrates in the different cells (total N removal of 5–99% in the whole experiment, and 18–99% in July 2007), with the planted cells performing significantly better than the control [21].

All of the concentrations were significantly affected by the different dilutions caused by evapotranspiration, which acted differently in the different cells. To take this effect into account, a comparison of the final mass of total N (TN) observed in the five cells is reported in Figure 3. The graph shows that the cells planted with *Typha* removed nearly all of the fed TN by the end of the second week, while the control only removed about 40% of the fed TN by the end of the entire month. The other planted cells showed intermediate performances.

Table 4. Measured and simulated evapotranspiration (ET) volumes (L).

		Outlet				Mean ET		Simulated ET	
July 2007:	Inlet	Week 1		Week 2		Week 1	Week 2	Week 1	Week 2
Carex e.	12	6.0	6.0	5.5	5.4	6.0	6.55	6.0	6.70
Juncus e.	12	5.0	6.0	5.3	4.9	6.5	6.90	6.0	6.50
Phragmites a.	12	5.0	5.0	3.4	4.5	7.0	8.05	7.0	7.80
Typha l.	12	2.0	4.0	0.2	0.2	9.0	11.80	8.6	10.20
Control	12	9.0	7.5	8.8	7.9	3.75	3.65	4.0	4.20
Dec. 2007:	Inlet	Week 1		Week 4		Week 1	Week 4	Week 1	Week 4
Carex e.	12	10.9	11.0	10.0	10.5	1.05	1.75	0.58	1.74

3.2 *Results of the simulations for July 2007*

The final calibrated ET_p values for the five cells are reported in the last column of Table 3, and the final values of the simulated water loss are compared with the goal values detected during the reference experiment in Table 4.

The vertical distribution of water transpiration withdrawal impinged on the biochemical processes by affecting the vertical distribution of soil water content.

After calibrating evapotranspiration, the nitrification process was calibrated by adjusting the value of the maximum specific growth of autotrophs μ_A, until a good simulation of the final ammonium concentration detected at the end of the first week of July 2007 was reached. The values of μ_A obtained at the end of the calibration for the five cells are reported in Table 3, while the simulated concentrations of ammonium are compared with the values detected in the reference experiment in Figure 4.

It should be noted that the approach of calibrating nitrification by adjusting the supply of oxygen did not allow for good simulations, because the presence of oxygen had a much higher inhibiting effect on denitrification than the effect of promotion of nitrification, thus leading to worse simulations of the overall N removal.

The last calibration stage was aimed at reaching the best simulation of the final value of nitrate concentration that was detected during the reference experiment. To reach this goal, the following strategies were attempted:

- adjusting the biochemical parameters governing the denitrification process: μ_H, b_H, K_S, $K_{O,H}$, K_{NO} and η_g (see Table 2 for an explanation of the terms);
- adjusting the aerobic conditions by calibrating the parameters governing the supply of oxygen: dispersion coefficient, global coefficient of oxygen exchange and tortuosity factor of the soil (this strategy required a further adjustment of nitrification);
- adjusting the provision of carbon for denitrification.

The first two strategies did not allow for a level of denitrification comparable to the one observed in the reference experiment to be reached. This was a clear demonstration that in the examined experiment the denitrification process had been strictly limited by the availability of a carbon source.

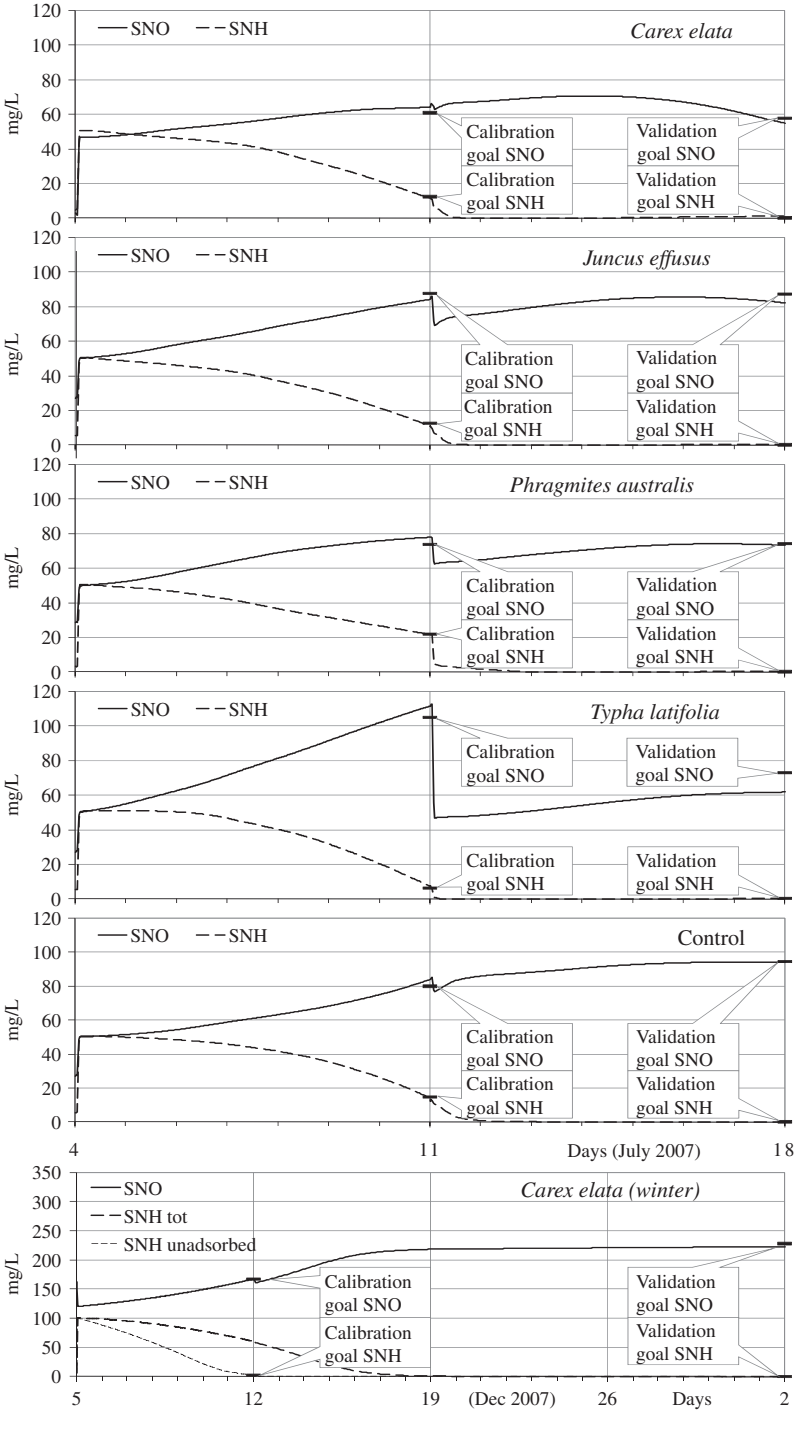

Figure 4. Simulations of nitrate N (SNO) and ammonia N (SNH) after calibration and validation, compared with concentrations from the reference experiments (goals).

We realised that an update of the model was necessary to simulate the provision of carbon exerted by the plants. To make this improvement, we first attempted a simplified method consisting of the addition of an artificial concentration of RBCOD to the feed water, the amount of which had to be defined for each plant by calibration. The carbon supply was therefore simulated by adding it to the entering water, whereas, in reality, the plants added carbon along the whole vertical distribution of the root apparatus, by the excretion of radical exudates.

This method did not result in good simulations of the experimental data because the provision of RBCOD in the entering water caused the excessive growth of a heterotrophic biomass located only in the top layer of the bed.

These results highlighted the fact that the vertical distribution of carbon supply plays an important role in the development of the denitrification process in the rhizosphere. Consequently, we implemented the new C supply module described previously, that simulated the input of an amount of RBCOD along the vertical of the bed, in proportion to the vertical distribution of the root density of the specific plant. The total amount could be set for each plant by calibration, whereas the vertical distribution of the root density was input as a rectangular, triangular or trapezoidal shape so as to resemble the real root distribution of each simulated plant.

This method obtained a good simulation of the final values of nitrates detected in the reference experiment, as shown in Figure 4. The values of carbon supply that obtained the best calibration results are reported in Table 3, and represent an interesting evaluation of carbon supply by decomposition of tissues and root exudates, as stated by several authors [28–31] but never estimated for specific wetland macrophytes. The average daily supply rates simulated during the calibration runs were also calculated, and are reported in Table 3. Differently than the supply rates r_{ECtot} of each plant, the daily supply rates are not constant, since they are affected by the vertical distribution of water content in the rhizosphere that decreases continuously as a function of evapotranspiration loss.

It should be noted that the control obtained a certain level of denitrification as well, although much lower than the planted cells. The low amount of carbon supply estimated by the model as being necessary for calibrating the observed value was attributed to the observed vegetal biofilm attached to the surface of the gravel in the top layer, with a triangular depth distribution.

In terms of the observed area-specific TN removal during the whole experiment, the best performance was obtained by the cell planted with *Typha* ($72\,g\,m^{-2}\,y^{-1}$) and the poorest by the control ($33.2\,g\,m^{-2}\,y^{-1}$) [21]. These values are very low when compared to the ordinary removal efficiency of subsurface flow constructed wetlands: an estimation of the TN removal based on the k-C* model [7] for horizontal SSF CWs under the same climatic conditions led to around $600\,g\,m^{-2}\,y^{-1}$. The main reason for this difference is that, in most cases, the fed wastewater in full-scale CWs contains all the carbon required for denitrification, whereas during this experiment the only available source was the endogenous supply from the plants.

The significant difference between the removal performances of the planted cells and the unplanted control was attributed to the fact that in the control the only carbon supply came from the minor vegetal biofilm observed on the surface of the top layer of gravel. This aspect confirms that the ability to supply carbon is a peculiar feature of plant species that can affect significantly the performance of CWs [32,33].

Table 5. Statistical goodness-of-fit evaluation parameters for the validation runs.

Parameter	Ammonium	Nitrate
Coefficient of determination R^2	0.68	0.96
Nash-Sutcliffe coefficient of efficiency E	0.30	0.96
Normalized mean bias error NMBE	−1.25	−0.0078
Normalized root mean square error NRMSE	1.989	0.1066

3.3 *Results of the simulations for December 2007*

Since the winter data-set of the experiment was not as complete as the one of July 2007, it was only possible to carry out a single winter simulation with *Carex elata* in December 2007, to assess the seasonal effect of this species. In this test, the input concentration of ammonium nitrate was doubled, and, because of the low evapotranspiration loss, the draining-refilling procedure was performed only at the end of the first week.

The results of the calibration and validation runs are shown in the last graph of Figure 4. In this case, the sorption of ammonium exerted by the gravel medium played an important role, demonstrated by the apparent lack of N balance observed between the first and fourth week. As well-described by Kadlec and Wallace [6], the gravel adsorbed significant amounts of ammonium that were released as nitrate after aeration due to the draining-refilling cycle at the end of the first week. The simulation of this process using the Freundlich isotherm provided by Sikora *et al.* as reported by Kadlec and Wallace [6] allowed us to reach a good simulation and validation of the winter data.

The values of carbon supply obtained from the best simulation of the winter experiment of *Carex e.* are reported in Table 3. A comparison with the summer results of the same species shows a decrease of 54% of carbon supply in winter.

3.4 *Goodness-of-fit evaluation of the validation runs*

The validation runs of the summer simulations were performed for the second week of July, while the winter simulation of *Carex elata* referred to the second, third and fourth weeks of December. The resulting time-distributions of ammonia and nitrate nitrogen are plotted in Figure 4, with the final observed concentrations (validation goals) also marked for a visual comparison.

To evaluate the goodness-of-fit of the validation results, the values of R^2, E, $NMBE$ and $NRMSE$ were calculated for the removal efficiency of ammonium and nitrates, and are reported in Table 5. All indices denote an acceptable fit of the simulated removal of nitrates, but a poor fit of the removal of ammonium.

However, the accuracy of the prediction of the removal of ammonium at the end of the validation weeks was strongly affected by the fact that the ammonium was removed almost completely, and the final values of concentration and mass were very low for both the measured and the simulated values. For this reason, very small differences significantly affected the comparisons.

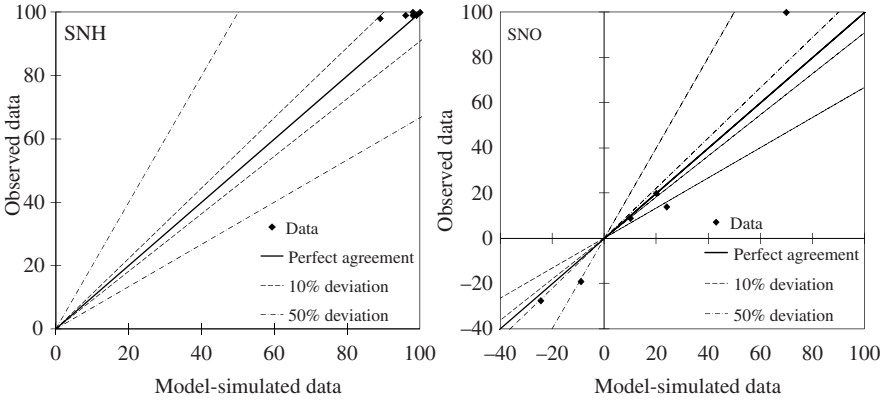

Figure 5. Comparison of measured and simulated removal efficiencies (%) for ammonium (SNH) and nitrates (SNO).

The last validation test is represented by the scatterplots of estimated-versus-observed data that are reported in Figure 5 for the removal efficiencies of ammonium and nitrates. The graphs show an acceptable fit for the removal efficiencies of both ammonium and nitrate, with the best result for ammonium, where all the data are included inside the cone of 10% deviation from perfect agreement.

4. Conclusions

The experimental tests highlighted that the different macrophytes showed significant differences in terms of the efficiency of nitrogen removal, especially in the removal of nitrates. The best simulation of the experimental results was obtained by including a carbon supply by the root exudates of the plants, the value of which was estimated in terms of overall amount and vertical distribution.

In summer, the best performing species was *Typha* (removing $72\,\mathrm{g\,TN\,m^{-2}\,y^{-1}}$), while the poorest performance was observed in the control ($33.2\,\mathrm{gTN\,m^{-2}\,y^{-1}}$). These values are very low when compared to the ordinary removal efficiency of SSF CWs, because in full scale CWs the fed wastewater normally contains all the carbon required for denitrification.

The unplanted control showed a lower level of denitrification, owing to a minor carbon supply attributed to the vegetal biofilm attached to the top layer of gravel.

The carbon supplied by plants ranged in summer from 5.76 to $7.02\,\mathrm{g/(m^2\,d)}$, while the control accounted for $5.11\,\mathrm{g/(m^2\,d)}$. In winter, the simulation for *Carex e.* showed a reduction of 54% of carbon supply and a significant influence of the adsorption of ammonium exerted by the gravel medium on the development of N removal.

The results of the tests enabled us to confirm that nitrification–denitrification processes play a major role in the removal of nitrogen in SSF CWs, and to provide estimations of the amount of endogenous carbon supplied by the plants used for the reference experiments. Since the wastewater used in the experiments was not realistic (no organic matter and excessive NO_3) and the cells were quite small, these values must be considered with care

and cannot be generalised, but this largely variable carbon supply is worth considering in the long-debated role of plants in CW performance.

The observed evapotranspiration losses were also simulated with a good approximation, and were shown to play a role in the development of biochemical processes by affecting the vertical distribution of soil water content.

As a last consideration, an analysis of the results of the validation runs demonstrated that the FITOVERT model performed acceptable simulations of the experimental data, despite the peculiar and difficult conditions of the experiment.

References

[1] EPA, *Manual Constructed Wetlands Treatment of Municipal Wastewaters* (USEPA Cincinnati, Ohio, USA, 2000).
[2] C.C. Tanner and J.P.S. Sukias, Water Sci. Technol. **48**, 331 (2003).
[3] T. Gschlöbl, C. Steinman, P. Schlypen, and A. Melzer, Water Res. **32**, 2639 (1998).
[4] EPA, *Subsurface Flow Constructed Wetlands for Waste Water Treatment: A Technology Assessment* (USEPA 832-R-93-008, 1993).
[5] M.L. Solano, P. Soriano, and M.P. Ciria, Biosyst. Engng. **87**, 109 (2004).
[6] R.H. Kadlec and S.D. Wallace, *Treatment Wetlands* (CRC Press, Boca Raton, USA, 2009).
[7] R.H. Kadlec, R.L. Knight, J. Vymazal, H. Brix, P. Cooper, and R. Haberl, *Constructed Wetlands for Pollution Control. IWA S. T. Report N. 8* (IWA Publishing, London, 2000).
[8] G. Langergraber, Sci. Total Environ. **380**, 210 (2007).
[9] D. Giraldi, M. de MichieliVitturi, and R. Iannelli, Environ. Modelling Software **25**, 633 (2010).
[10] G. Langergraber, D. Giraldi, J. Mena, D. Meyer, M. Pena, A. Toscano, A. Brovelli, and E. Asuman Korkusuz, Sci. Total Environ. **407**, 3931 (2009).
[11] A. Brovelli, F. Malaguerra, and D.A. Barry, Environ. Modelling Software **24**, 611 (2009).
[12] Y. Lin, S. Jing, T. Wang, and D. Lee, Environ. Pollut. **119**, 413 (2002).
[13] A. Wieβner, U. Kappelmeyer, P. Kuschk, and M. Kästner, Water Res. **39**, 248 (2005).
[14] N.P. Hume, M.S. Fleming, and A.J. Horne, Soil Sci. Soc. Am. J. **66**, 1706 (2002).
[15] R.M. Gersberg, B.V. Elkins, and C.R. Goldman, Water Res. **17**, 1009 (1983).
[16] R. Iannelli, L. Iacopini, P. Peruzzi, and A. Scarselli, Proceedings of the VI SIBESA International Conference, Vitoria, BRA, 2002.
[17] P.S. Burgoon, Water Sci. Technol. **44**, 163 (2001).
[18] L.D. Bailey, Can. J. Soil Sci. **56**, 79 (1976).
[19] H. Brix, Water Sci. Technol. **29**, 71 (1994).
[20] M. Greenway, Water Sci. Technol. **48**, 121 (2003).
[21] M. Salvato and M. Borin, Ecol. Engng. **36**, 1222 (2010).
[22] APHA, *Standard Methods*, 19th ed. (American Public Health Association, Washington DC, 1995).
[23] M. Henze, C.P.L. Grady Jr, W. Gujer, G.v.R. Marais, and Y. Matsuo, *Activated Sludge Model No. 1. IAWPRC S. T. Report N.1* (IAWPRC, London, 1987).
[24] U. Jeppsson, *Modelling aspects of wastewater treatment processes* (Lund Institute of Technology, Department of Industrial Electrical Engineering and Automation, ISBN 91-88934-00-4, www.iea.lth.se/publications/Theses/LTH-IEA-1010.pdf, 1996).
[25] D.R. Legates and G.J. McCabe Jr, Water Res. **35**, 233 (1999).
[26] J.E. Nash and J.V. Sutcliffe, J. Hydrol. **10**, 282 (1970).
[27] Y. Jiang, Appl. Energy **86**, 1458 (2009).
[28] M. Biondini, D.A. Klein, and E.F. Redente, Soil Biol. Biochem. **20**, 477 (1988).

[29] J.C. Neff and G.P. Asner, Ecosystems **4**, 29 (2001).
[30] S. Lu, H. Hu, Y. Sun, and J. Yang, J. Environ. Sci. **21**, 1036 (2009).
[31] L. Kong, Y.B. Wang, L.N. Zhao, and Z.H. Chen, Chemosphere **76**, 601 (2009).
[32] R.H. Kadlec, Ecol. Engng. **33**, 126 (2008).
[33] F. Morari and L. Giardini, Ecol. Engng. **35**, 643 (2008).